Electric Power Systems Research 84 (2012) 45–57

Contents lists available at SciVerse ScienceDirect

Electric Power Systems Research

journal homepage: www.elsevier.com/locate/epsr

Linear power flow *V*-theta

Ailson P. de Moura[a,*], Adriano A.F. de Moura[b], D.S. Oliveira Jr.[a], E.J. Fernandes[a]

[a] Department of Electrical Engineering, Federal University of Ceara Technology Center, Pici Fortaleza-CE, CEP: 59.810-321, Brazil
[b] Department of Environmental Science and Technology, Federal Rural University of Semi-Arid, Av. Francisco Mota, 572 Bairro Costa e Silva, Mossoró-RN, CEP: 59.625-900, Brazil

ARTICLE INFO

Article history:
Received 26 May 2011
Received in revised form
23 September 2011
Accepted 27 September 2011
Available online 28 October 2011

Keywords:
Linear model
DC power flow
Power flow
Contingency analysis

ABSTRACT

This paper presents a new linear active power flow solution method. The new linear active power flow presents a better performance to calculate MW power flows, as opposed to MW flows, calculated in classical model with a DC power flow. The aforesaid proposed method is based on a decoupling principle. Therefore, the voltage angles and voltage magnitudes are calculate in decoupled forms. A complete demonstration of the proposed method is presented. The algorithm of new method has been tested by extensive numerical studies. This paper gives details of the method's performance on various classical systems. All the results are compared with those from the Newton–Raphson power flow and classical DC power flow.

1. Introduction

The power flow calculation is one of the most commonly used tools in power system engineering. For that reason, the history of power flow calculation is a relatively long one. Since the invention and widespread of computers, in the 1950s and 1960s, many methods for solving the power flow problem have been developed [1].

The classical direct current (DC) power flow technique calculates only real power flows within power systems networks. The DC power flow method was especially attractive in the middle of the twentieth century, when computer access was expensive, and there was a real need to reduce central processing unit (CPU) time on all computational activities. Presently, the DC power flow method is used extensively in power system analysis and power market applications [2,3]. Several examples are presented herewith: (A) Contingency Analysis – Contingency analysis is the focal point in evaluating power system security. The DC power flow method is preferred in this analysis [4]; (B) Calculation of Power Transfer Distribution Factors (PTDF) – The PTDF represents the sensitivities of lines flow with respect to generation changes [4]. The PTDFs are used in transmission congestion management applications and also in the calculation of Locational Marginal Price (LMP) [5,6]; (C) Calculation of Line Outage Distribution Factors (LODF) – The LODF measures the sensitivity of a line flow against the removal of another line. The LODF is used in the calculation of available transfer capability (ATC), as well as developing constraints for SPD (Scheduling, Pricing and Dispatch) and Security Constrained Unit Commitment (SCUC) programs [5,7,8]; (D) Transmission Interchange Limit Analysis – The Transfer Limit Table Generator (TLTG) and POLY analyses are transmission interchange limit analysis functions in Power System Simulator for Engineering (PSS/E) [7], which estimate the import/export limits between two areas ("study system" and "opposing system") using linearized network model. The POLY function differs from the TLTG in that it considers simultaneous generation shifts in two opposing systems to maximize study system import/export; (E) Market Clearing Engine (MCE) – The Scheduling, Pricing, and Dispatch (SPD), Security Constrained Unit Commitment (SCUC) and Simultaneous Feasibility Test/Network Application (SFT/NA) are core programs of an MCE. The SPD and SCUC are security constrained optimal power flow programs, often based on the linear DC power flow equations. The objective is to minimize the total cost of generation and reserves, subject to a set of constraints including power balance, ancillary services, resources operating limits and transmission security constraints; (F) Financial Transmission Right – Financial transmission right (FTR), also known as firm transmission right, is a financial instrument for hedging risks from transmission congestion costs on constrained lines [9]. A linear programming (LP) problem is formulated to clear the FTR auction. The objective function of the LP problem is to maximize the revenues from FTR. The thermal limits of the transmission lines are formulated as power flow constraints of

* Corresponding author. Tel.: +55 85 32413528.
E-mail address: ailson@ufc.br (A.P. de Moura).

0378-7796/$ – see front matter © 2011 Elsevier B.V. All rights reserved.
doi:10.1016/j.epsr.2011.09.020

the LP problem. Others developments in this area are comparisons of MW flows obtained from DC and AC power flow solutions [10], and methods that try to account for the Mvar flows that are absent from DC models [11].

The advantages of a DC model are as follows:

(a) Its solutions are non-iterative, reliable and unique;
(b) Its methods and software are relatively simple;
(c) Its models can be solved and optimized efficiently, particularly in the demanding area of contingency analysis;
(d) Its network data is minimal and relatively easy to obtain;
(e) Its linearity fits the economic theory on which much of transmission-oriented market design is based;
(f) Its approximated MW flows are reasonably accurate, at least for the heavily loaded branches that might constrain system operation.

These are powerful attractions and, general, items (a)–(e) are mostly valid. However, it is well known that the DC power flow method offers only approximate solutions, especially when the R/X ratios for transmission lines are large and bus voltages are highly non-uniform. This inaccuracy leads to compromised system reliability when used in system security analysis, and can have economic consequences by changing the LMP in security constrained economic dispatch or FTR awards in FTR auctions [8].

The method described in this paper presents a better performance to calculate MW power flows than MW flows calculates in classical model of a DC power flow. Great importance is presented to the fact that this proposed method, is derived from some theoretical bases. The method is based on decoupling principles, and it uses a procedure that solves the voltage angles and voltage magnitudes in decoupled forms. The new method can calculate active and reactive power flows. However, due to page limit, the reactive power flows will be presented and validated in future paper.

The paper is organized as follows: Firstly, a complete demonstration of the proposed method is presented, inclusive with numerical examples; all the necessary approximations and details required by proposed method are identified. Test results are presented with some relevant conclusions duly reported.

2. Development of the linear power flow *V*-theta

Consider expressions for the active power flows in a transmission line. These expressions are explained briefly in Appendix A, where a summary of the DC power flow is presented. The following approximations are made:

$$V_k^2 \cong factorV_k \tag{1}$$

$$V_m^2 \cong factorV_m \tag{2}$$

$$V_k V_m \cong factorV1_{km} \tag{3}$$

$$\sin\ \theta_{km} \cong \theta_{km} \tag{4}$$

$$\cos\ \theta_{km} \cong 1 \tag{5}$$

Then, the linearized expressions for the active power flow in a transmission line are as follows:

$$P_{km}^{LIN} = factorV_k g_{km} - factorV1_{km} g_{km} - factorV1_{km} b_{km} \theta_{km} \tag{6}$$

$$P_{mk}^{LIN} = factorV_m g_{km} - factorV1_{mk} g_{km} + factorV1_{mk} b_{km} \theta_{km} \tag{7}$$

where the superscript "LIN" means linearized.

g_{km} and b_{km} are respectively series conductance and series susceptance.

$$factorV_k = cV_k + d$$

$$factorV_m = eV_m + g$$

c, d, e, and g are constants, i.e. the $factorV_k$ and $factorV_m$ are approximated as linear functions; where V_k and V_m are numerical values of voltage magnitudes read from the data file.

$factorV1_{km}$ is the linear approximation of the tangent plane to a surface at a point stays close to the surface near the point [12]. At point (a, b) $factorV1_{km} = f(x, y) = f(a, b) + f_x(a, b)(x - a) + f_y(a, b)(y - b)$.

The $factorV_k$ and $factorV_m$ are calculated at intervals of 0.005 p.u. The $factorV1_{km}$ is calculated at point $a = V_k + k$ and $b = V_m + k$ both in p.u., where k is a constant. Therefore, the local linearization of $f(x, y) = xy$ at point (a, b) is

$$factorV1_{km} = (V_m + k)x + (V_k + k)y - V_k V_m - kV_k - kV_m - k^2 \tag{8}$$

When $x = V_k$ and $y = V_m$ in Eq. (8), $factorV1_{km}$ is

$$factorV1_{km} = V_k V_m - k^2 \tag{9}$$

The calculation of the voltage angles and voltage magnitudes, in a linearized form, are made as follow: Two equations of active power mismatches (ΔP) and two equations of power reactive mismatches (ΔQ), are written in matrix form and they are linearized. The first two equations have ΔP and ΔQ with the voltage angles as unknowns. The next two equations present ΔP and ΔQ with voltage magnitudes as unknowns. The four equations form an overdetermined system of linear equations, which is solved by a mathematical procedure already known [13,14].

The others assumptions made within the linear power flow V-theta technique are as follows:

1. All busbar *PQ* voltage magnitudes initializes at 1.0 p.u.
2. The voltage magnitudes in the *PV* buses are kept in the duly specified values.
3. All busbar voltage angles initializes at zero radian.
4. Omit all effects from phase shift transformers.
5. The taps of in-phase transformers are being kept in the calculations for the formation of all equations.
6. The equations of active power mismatches are used at buses type *PV* and *PQ*
7. The equations of reactive power mismatches are used only at buses type *PQ*.

The shunts in elements of susceptance B_{kk} of all equations are omitted and they are included only in the equations of reactive power mismatches in each bus as reactive power generated, i.e.:

$Q_k^G = \sum_{m\in k}(b_{km}^{sh}/2)$ factor $V_k + b_k^{shunt}$factor V_k, where b_{km}^{sh} is shunt admittance of the line and b_k^{shunt} is shunt capacitor bank or shunt reactor bank. The other variables have been defined previously.

2.1. Development of the equations linearized of ΔP and ΔQ with the voltage angles as unknowns.

Consider the basic equations of power flow

$$\Delta P_k = P_k^{sp} - V_k\sum_{m=1}^{NB} V_m(G_{km}\ \cos\ \theta_{km} + B_{km}\ \sin\ \theta_{km}) = 0 \tag{10}$$

$$\Delta Q_k = Q_k^{sp} - V_k\sum_{m=1}^{NB} V_m(G_{km}\ \sin\ \theta_{km} - B_{km}\ \cos\ \theta_{km}) = 0 \tag{11}$$

where NB is the number of buses of the network.

$\Delta P_k + j\Delta Q_k$, complex power mismatch at bus k; $G_{km} + jB_{km}$, (k, m)th element of bus admittance matrix; θ_k, V_k, voltage angle, magnitude at bus k; θ_{km}, $\theta_k - \theta_m$; $P_k^{sp} + jQ_k^{sp}$, scheduled complex power at bus k.

The approximations considered in Eqs. (4) and (5) are used in Eqs. (10) and (11). Thereafter, the expressions (10) and (11) are modified as:

$$\Delta P_k \cong P_k^{sp} - V_k^2 G_{kk} - V_k \sum_{\substack{m=1\\ m\neq k}}^{NB} V_m(G_{km} + B_{km}\theta_{km}) \cong 0 \tag{12}$$

$$\Delta Q_k \cong Q_k^{sp} + V_k^2 B_{kk} + V_k \sum_{\substack{m=1\\ m\neq k}}^{NB} V_m(B_{km} - G_{km}\theta_{km}) \cong 0 \tag{13}$$

Linear power flow V-theta initializes voltage angles as zero radian. Therefore, when the angles are equal to zero, the terms of Eqs. (12) and (13) that contains angular differences, do not influence the numerical values of mismatches of active and reactive power. Therefore, Eqs. (12) and (13) can be written as follows:

$$\Delta P_k \cong P_k^{sp} - V_k^2 G_{kk} - V_k \sum_{\substack{m=1\\ m\neq k}}^{NB} V_m G_{km} \cong V_k \sum_{\substack{m=1\\ m\neq k}}^{NB} V_m B_{km}\theta_{km} \cong 0 \tag{14}$$

$$\Delta Q_k \cong Q_k^{sp} + V_k^2 B_{kk} + V_k \sum_{\substack{m=1\\ m\neq k}}^{NB} V_m B_{km} \cong V_k \sum_{\substack{m=1\\ m\neq k}}^{NB} V_m G_{km}\theta_{km} \cong 0 \tag{15}$$

In matrix form:

$$[\Delta P_k] \cong [J1][\Delta\theta_k] \tag{16}$$

$$[\Delta Q_k] \cong [J3][\Delta\theta_k] \tag{17}$$

However, the bus number 1 is considered as swing bus. Then $k = 2, 3, \ldots, NB$. Where

$$[\Delta\theta_k] = [\theta_k] - [0]$$

$$[J1] = \begin{cases} J1_{km} = V_k V_m(-B_{km}) \\ J1_{kk} = \sum_{\substack{m=1 \\ m\neq k}}^{NB} V_k V_m B_{km} \end{cases} \qquad [J3] = \begin{cases} J3_{km} = -V_k V_m G_{km} \\ J3_{kk} = \sum_{\substack{m=1 \\ m\neq k}}^{NB} V_k V_m G_{km} \end{cases} \tag{18}$$

The dimensions of the respective matrices $[J1]$ and $[J3]$ are respectively $(NPQ + NPV) \times (NPQ + NPV)$ and $(NPQ) \times (NPQ + NPV)$, where NPQ is the number of buses type PQ and NPV is the number of buses type PV occur. Since those assumptions 6 and 7 are considered.

The linearization of the equations is completed as follow. Using the approximations made in Eqs. (1)–(5) at power mismatches Eqs. (10) and (11) and using approximations made in (1)–(3) at Eq. (18):

$$\Delta P_k^{LIN} = P_k^{sp} - factorV_k G_{kk} - \sum_{\substack{m=1 \\ m\neq k}}^{NB} factorV1_{km}(G_{km} + B_{km}\theta_{km}) \tag{19}$$

$$\Delta Q_k^{LIN} = Q_k^{sp} - factorV_k(-B_{kk}) - \sum_{\substack{m=1 \\ m\neq k}}^{NB} factorV1_{km}(G_{km}\theta_{km} - B_{km}) \tag{20}$$

Eqs. (19) and (20) linearized in matrix form are represented as follows:

$$[\Delta P_k]^{LIN} = [J1]^{LIN}[\Delta\theta_k]^{LIN} \tag{21}$$

$$[\Delta Q_k]^{LIN} = [J3]^{LIN}[\Delta\theta_k]^{LIN} \tag{22}$$

where $[\Delta\theta_k]^{LIN} = [\theta_k]^{LIN} - [0]$

$$[J1]^{LIN} = \begin{cases} J1_{km}^{LIN} = factorV1_{km}(-B_{km}) \\ J1_{kk}^{LIN} = \sum_{\substack{m=1 \\ m\neq k}}^{NB} factorV1_{km} B_{km} \end{cases} \qquad [J3]^{LIN} = \begin{cases} J3_{km}^{LIN} = -factorV1_{km} G_{km} \\ J3_{kk}^{LIN} = \sum_{\substack{m=1 \\ m\neq k}}^{NB} factorV1_{km} G_{km} \end{cases} \tag{23}$$

2.2. Development of the equations linearized of ΔP and ΔQ with the voltage magnitudes as unknowns

The approximations considered in Eqs. (4) and (5) are used again in Eqs. (10) and (11). Then, the expressions (10) and (11) are modified as such:

$$\Delta P_k \cong P_k^{sp} - V_k \sum_{m=1}^{NB} V_m B_{km}\theta_{km} \cong V_k \sum_{m=1}^{NB} V_m G_{km} \tag{24}$$

$$\Delta Q_k \cong Q_k^{sp} - V_k \sum_{m=1}^{NB} V_m G_{km}\theta_{km} \cong V_k \sum_{m=1}^{NB} V_m(-B_{km}) \tag{25}$$

In the following equations, the shunts are omitted, and the taps of in-phase transformers are kept. Thus, Eqs. (26) and (27) are approximately equal to a zero.

$$V_k \sum_{m=1}^{NB} G_{km} \cong 0 \tag{26}$$

$$V_k \sum_{m=1}^{NB} (-B_{km}) \cong 0 \tag{27}$$

Subtracting Eq. (26) on right side of Eq. (24) and subtracting Eq. (27) on right side of Eq. (25) and rearranging the terms we obtain

$$\Delta P_k \cong P_k^{sp} - V_k \sum_{m=1}^{NB} V_m B_{km} \theta_{km} \cong V_k \sum_{m=1}^{NB} G_{km}(V_m - 1) \tag{28}$$

$$\Delta Q_k \cong Q_k^{sp} - V_k \sum_{m=1}^{NB} V_m G_{km} \theta_{km} \cong V_k \sum_{m=1}^{NB} (-B_{km})(V_m - 1) \tag{29}$$

The linearization of Eq. (28) and (29) is completed as follow: first the PV buses and PQ buses are separated in summation of the right side. Then, the linear approximation of the tangent plane to a surface at a point, staying close to the surface near the point, is made using Eq. (9).

$$V_k \sum_{m=1}^{NB} G_{km}(V_m - 1) = \sum_{\substack{m=1 \\ m \in PV \\ REF}}^{NB} factorV1_{km} G_{km} - V_k \sum_{\substack{m=1 \\ m \in P \\ REFV}}^{NB} G_{km} + \sum_{\substack{m=1 \\ m \in PQ}}^{NB} V_k G_{km}(V_m - 1) - k^2 \sum_{\substack{m=1 \\ m \in PQ}}^{NB} G_{km} \tag{30}$$

$$V_k \sum_{m=1}^{NB} (-B_{km})(V_m - 1) = \sum_{\substack{m=1 \\ m \in PV \\ REF}}^{NB} factorV1_{km}(-B_{km}) - V_k \sum_{\substack{m=1 \\ m \in PV \\ REF}}^{NB} (-B_{km}) + \sum_{\substack{m=1 \\ m \in PQ}}^{NB} V_k(-B_{km})(V_m - 1) - k^2 \sum_{\substack{m=1 \\ m \in PQ}}^{NB} (-B_{km}) \tag{31}$$

Substituting Eqs. (30) and (31) in Eqs. (28) and (29) and rearranging the terms:

$$\Delta P_k \cong P_k^{sp} - \sum_{m=1}^{NB} factorV1_{km} B_{km} \theta_{km} - \sum_{\substack{m=1 \\ m \in PV \\ REF}}^{NB} factorV1_{km} G_{km} + \sum_{\substack{m=1 \\ m \in PV \\ REF}}^{NB} V_k G_{km} + k^2 \sum_{\substack{m=1 \\ m \in PQ}}^{NB} G_{km} \cong V_k \sum_{\substack{m=1 \\ m \in PQ}}^{NB} G_{km} \Delta V_m \tag{32}$$

$$\Delta Q_k \cong Q_k^{sp} - \sum_{m=1}^{NB} factorV1_{km} G_{km} \theta_{km} - \sum_{\substack{m=1 \\ m \in PV \\ REF}}^{NB} factorV1_{km}(-B_{km}) - V_k \sum_{\substack{m=1 \\ m \in PV \\ REF}}^{NB} (-B_{km}) + k^2 \sum_{\substack{m=1 \\ m \in PQ}}^{NB} (-B_{km}) \cong V_k \sum_{\substack{m=1 \\ m \in PQ}}^{NB} (-B_{km}) \Delta V_m \tag{33}$$

where

$m \in PV, REF$ The bus m belongs to the set of PV buses and swing bus.

$m \in PQ$ The bus m belongs to the set of PQ buses.

$$\Delta V_m = V_m - 1$$

Linear power flow V-theta initializes the voltage magnitudes of buses type PQ as 1.0 p.u. Later on, the terms on the right side of Eqs. (32) and (33) are null. Therefore, Eqs. (19) and (32) are approximately equal. Same comments apply to Eqs. (20) and (33). Thus, Eqs. (32) and (33) can be written as follows:

$$\Delta P_k^{LIN} \cong V_k \sum_{\substack{m=1 \\ m \in PQ}}^{NB} G_{km} \Delta V_m \cong 0 \tag{34}$$

$$\Delta Q_k^{LIN} \cong \sum_{\substack{m=1 \\ m \in PQ}}^{NB} (-B_{km}) \Delta V_m \cong 0 \tag{35}$$

In matrix form:

$$[\Delta P_k]^{LIN} \cong [J2]^{LIN} [\Delta V_k]^{LIN} \tag{36}$$

$$[\Delta Q_k]^{LIN} \cong [J4]^{LIN} [\Delta V_k]^{LIN} \tag{37}$$

where

$$[\Delta V_k]^{LIN} = [V_k]^{LIN} - [1]$$

$$[J2]^{LIN} = \begin{cases} J2_{km}^{LIN} = V_k G_{km} \\ \\ J2_{kk}^{LIN} = V_k G_{kk} \end{cases} \tag{38}$$

$$[J4]^{LIN} = \begin{cases} J4_{km}^{LIN} = V_k(-B_{km}) \\ \\ J4_{kk}^{LIN} = V_k(-B_{kk}) \end{cases}$$

The dimensions of the respective matrices $[J2]^{LIN}$ and $[J4]^{LIN}$ are respectively (NPQ + NPV) × (NPQ) and (NPQ) × (NPQ). Since those assumptions 6 and 7 are considered.

2.3. Solution of the overdetermined system of linear equations

An overdetermined system of linear equations is obtained, when the set of linear equations (22), (23), (36) and (37) are used to calculate the voltage angles and the voltage magnitudes. Then, the process to calculate the voltage angles and voltage magnitudes linearized is completed as follows.

Eq. (23) is multiplied by $[J2]^{LIN}([J4]^{LIN})^{-1}$

$$[J2]^{LIN}([J4]^{LIN})^{-1}[\Delta Q_k]^{LIN} = [J2]^{LIN}([J4]^{LIN})^{-1}[J3]^{LIN}[\Delta\theta_k]^{LIN} \tag{39}$$

Subtracting Eq. (22) minus Eq. (39):

$$[\Delta P_k]^{LIN} - [J2]^{LIN}([J4]^{LIN})^{-1}[\Delta Q_k]^{LIN} = \{[J1]^{LIN} - [J2]^{LIN}([J4]^{LIN})^{-1}[J3]^{LIN}\}[\Delta\theta_k]^{LIN} \tag{40}$$

Solve Eq. (40) for voltage angles:

$$[\Delta\theta_k]^{LIN} = \{[J1]^{LIN} - [J2]^{LIN}([J4]^{LIN})^{-1}[J3]^{LIN}\}^{-1}\{[\Delta P_k]^{LIN} - [J2]^{LIN}([J4]^{LIN})^{-1}[\Delta Q_k]^{LIN}\} \tag{41}$$

In compact form:where

$$\left[\Delta\theta_k\right]^{LIN} = \left[[A1]^{LIN}\right]^{-1}\left[\Delta P_{eq}\right]^{LIN} \tag{42}$$

$$[A1]^{LIN} = \left[[J1]^{LIN} - [J2]^{LIN}([J4]^{LIN})^{-1}[J3]^{LIN}\right] \tag{43}$$

$$\left[\Delta P_{eq}\right]^{LIN} = \left[[\Delta P_k]^{LIN} - [J2]^{LIN}([J4]^{LIN})^{-1}[\Delta Q_k]^{LIN}\right] \tag{44}$$

Eq. (42) is used to calculate the voltage angles.

Voltage magnitudes are calculated as follows: Eq. (36) is multiplied by $[J3]^{LIN}([J1]^{LIN})^{-1}$

$$[J3]^{LIN}([J1]^{LIN})^{-1}[\Delta P]^{LIN} = [J3]^{LIN}([J1]^{LIN})^{-1}[J2]^{LIN}[\Delta V_k]^{LIN} \tag{45}$$

Subtracting Eq. (37) minus Eq. (45)

$$[\Delta Q_k]^{LIN} - [J3]^{LIN}([J1]^{LIN})^{-1}[\Delta P_k]^{LIN} = \{[J4]^{LIN} - [J3]^{LIN}([J1]^{LIN})^{-1}[J2]^{LIN}\}[\Delta V_k]^{LIN} \tag{46}$$

Solve Eq. (46) for voltage magnitudes:

$$[\Delta V_k]^{LIN} = \{[J4]^{LIN} - [J3]^{LIN}([J1]^{LIN})^{-1}[J2]^{LIN}\}^{-1}\{[\Delta Q_k]^{LIN} - [J3]^{LIN}([J1]^{LIN})^{-1}[\Delta P_k]^{LIN}\} \tag{47}$$

In compact form:where

$$[\Delta V_k]^{LIN} = [[A2]^{LIN}]^{-1}[\Delta Q_{eq}]^{LIN} \tag{48}$$

$$[A2]^{LIN} = [[J4]^{LIN} - [J3]^{LIN}([J1]^{LIN})^{-1}[J2]^{LIN}] \tag{49}$$

$$[\Delta Q_{eq}]^{LIN} = [[\Delta Q_k]^{LIN} - [J3]^{LIN}([J1]^{LIN})^{-1}[\Delta P_k]^{LIN}] \tag{50}$$

Eq. (48) is used in the calculation of voltage magnitudes.

Fig. 1 shows the basic flowchart of the method, where DP is the power active mismatch and DQ is the power reactive mismatch.

Hence, a numerical example is presented to clarify the new linear active power flow. The results of the enclosed tables herewith, are calculated by the following equations:

$$P_{error} = (P_{AC} - P^{LIN}) \tag{51}$$

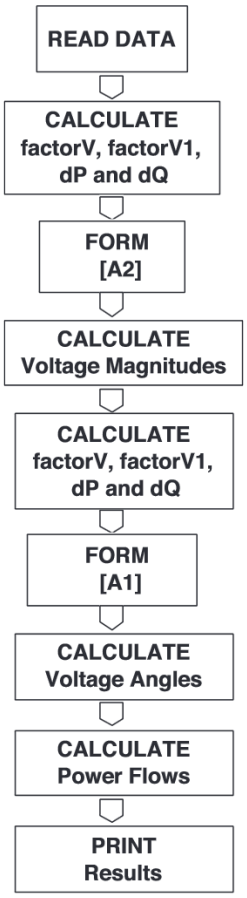

Fig. 1. Basic flowchart of the linear power flow V-theta.

Table 1
Bus data system of 4 buses.

Bus No.	Type	Voltage (p.u.)	Phase angle (rd)	Generator *P* (p.u.)	Generator *Q* (p.u.)	Load *P* (p.u.)	Load *Q* (p.u.)
1	Swing	1.0	0.0	0.0	0.0	0.0	0.0
2	PQ	1.0	0.0	0.0	0.0	0.5	0.2
3	PQ	1.0	0.0	0.0	0.0	0.6	0.1
4	PV	1.05	0.0	0.6	0.0	0.0	0.0

$$PP_{error} = \frac{(P_{AC} - P^{LIN})}{P_{AC}} \times 100\% \tag{52}$$

$$PA_{error} = \sum abs(P_{AC} - P^{LIN}) \tag{53}$$

where P_{error} is the difference between AC power flow and linear decoupled power flow/DC power flow (MW); PP_{error} is the active power flow percent error; PA_{error} is the sum of absolute values of P_{error}

2.4. Simulation of a small system

In this particular item, we will give a numerical example to illustrate the linear power flow V-theta. We will take as example, the four-bus system, whose data are shown in Tables 1 and 2. These admittance series of the five lines are in p.u.

The calculations follow the basic flowchart.

Table 2
Branch data – system of 4 buses.

From bus	To bus	Serie admittance (p.u.)
1	3	0.2-*J*3
1	4	0.5-*J*5
2	3	1-*J*3
2	4	0.5-*J*5
3	4	1-*J*3

1. Calculation of $factorV_k$ and $factorV1_{km}$

$$[V_k] = \begin{bmatrix} 1.000_1 \\ 1.000_2 \\ 1.000_3 \\ 1.050_4 \end{bmatrix} \quad [factorV1_{km}] = \begin{bmatrix} 0.999999_{1-3} \\ 1.049999_{1-4} \\ 0.999999_{2-3} \\ 1.049999_{2-4} \\ 1.049999_{3-4} \end{bmatrix} \quad [factorV_k] = \begin{bmatrix} 1.0000_1 \\ 1.0000_2 \\ 1.0000_3 \\ 1.1025_4 \end{bmatrix}$$

Example: linear function

$$factorV_4 = 2.095001 \times V_4 - 1.097251 = 2.095001 \times 1.05 - 1.097251 = 1.10250005$$

Equation of tangent plane (8): $factorV1_{2-4} = (1.05 + 0.001) \times 1 + (1 + 0.001) \times 1.05 - 1.052051 = 1.0499999$

2. Calculation of linearized power mismatches (p.u.): Eqs. (19) and (20).

$$[\Delta P]^{LIN} = \begin{bmatrix} -0.4750 \\ -0.5500 \\ 0.4950 \end{bmatrix} \quad [\Delta Q]^{LIN} = \begin{bmatrix} 0.0499 \\ 0.0499 \end{bmatrix}$$

Example: Eqs. (19) and (20).

$$\Delta P_2^{LIN} = P_k^{sp} - factorV_2 G_{22} - (factorV1_{2-1} G_{21} + factorV1_{2-3} G_{23} + factorV1_{2-4} G_{24})$$

$$\Delta Q_2^{LIN} = Q_k^{sp} - factorV_2(-B_{22}) - (factorV1_{2-1}(-B_{21}) + factorV1_{2-3}(-B_{23}) + factorV1_{2-4}(-B_{24}))$$

Since voltage angles are null. Therefore:

$$\Delta P_2^{LIN} = 0 - 0.5 - 1 \times 1.5 - (0 + 0.999999 \times (-1) + 1.049999 \times (-0.5)) = -0.4750$$

$$\Delta Q_2^{LIN} = 0 - 0.2 - 1 \times (-(-8)) - (0 + 0.999999 \times (-3) + 1.049999 \times (-5)) = -0.0499$$

3. Calculation of the matrices $[J1]$, $[J2]$, $[J3]$ and $[J4]$: Eqs. (21) and (38).

$$[J1] = \begin{bmatrix} 8.249992 & -2.999997 & -5.249995 \\ -2.999997 & 9.149991 & -3.149997 \\ -5.249995 & -3.149997 & 13.649987 \end{bmatrix}, \quad [J2] = \begin{bmatrix} 1.500000 & -1.000000 \\ -1.000000 & 2.200000 \\ -0.525000 & -1.050000 \end{bmatrix}$$

$$[J3] = \begin{bmatrix} -1.524999 & 0.999999 & 0.524999 \\ 0.999999 & -2.249998 & 1.049999 \end{bmatrix}, \quad [J4] = \begin{bmatrix} 8.000000 & -3.000000 \\ -3.000000 & 9.000000 \end{bmatrix}$$

Example:

$$J1_{23}^{LIN} = factorV1_{23}(-B_{23}) = 0.999999 \times (-3) = 2.999997, \quad J1_{33}^{LIN} = factorV1_{31} B_{31} + factorV1_{32} B_{32} + factorV1_{34} B_{34}$$
$$= 0.999999 \times 3 + 0.999999 \times 3 + 1.049999 \times 3 = 9.149991$$

$$J2_{42}^{LIN} = V_4 G_{42} = 1.05(-0.5) = -0.525, \quad J2_{22} = V_2 G_{22} = 1 \times 1.5 = 1.5$$

$$J3_{34}^{LIN} = -factorV1_{34} G_{34} = -1.049999(-1) = 1.049999 \quad J3_{22}^{LIN} = factorV1_{21} G_{21} + factorV1_{23} G_{23} + factorV1_{24} G_{24}$$
$$= 0 + 0.999999(-1) + 1.049999(-0.5) = 1.524999$$

$$J4_{32}^{LIN} = V_3(-B_{32}) = 1(-3) = -3, \quad J4_{33}^{LIN} = V_3(-B_{33}) = 1(-(-9)) = 9$$

4. Calculation of voltage magnitudes (p.u.): Eq. (48).

$$[V_k] = \begin{bmatrix} 1.0000_1 \\ 0.9974_2 \\ 0.9946_3 \\ 1.0500_4 \end{bmatrix}$$

Table 3
Maximum error – sum of errors (MW).

Test system 4 buses	DC power flow	Linear power flow V-theta
Max(abs(PP_{error})) (%)	14.37	5.14
PA_{error} (MW)	4.14	1.68
Max(abs(P_{error})) (MW)	2.57	0.92

Max(abs) is the maximum absolute value.

5. Calculation of $factorV_k$ and $factorV1_{km}$

$$[factorV_k] = \begin{bmatrix} 1.0000_1 \\ 0.9948_2 \\ 0.9892_3 \\ 1.1025_4 \end{bmatrix}, \quad [factorV1_{km}] = \begin{bmatrix} 0.994592566_{1-3} \\ 1.049999000_{1-4} \\ 0.991990089_{2-3} \\ 1.047251544_{2-4} \\ 1.044322244_{3-4} \end{bmatrix}$$

6. Calculation of linearized power mismatches (p.u.): Eqs. (19) and (20).

$$[\Delta P]^{LIN} = \begin{bmatrix} -0.4766 \\ -0.5411 \\ 0.4879 \end{bmatrix}, \quad [\Delta Q]^{LIN} = \begin{bmatrix} 0.0540 \\ 0.0897 \end{bmatrix}$$

7. Calculation of the matrices [J1], [J2], [J3] and [J4]: Eqs. (21) and (38).

$$[J1] = \begin{bmatrix} 8.2122 & -2.9759 & -5.2362 \\ -2.9759 & 9.0927 & -3.1330 \\ -5.2362 & -3.1330 & 13.6192 \end{bmatrix}, \quad [J2] = \begin{bmatrix} 1.4961 & -0.9974 \\ -0.9946 & 2.1881 \\ -0.5250 & -1.0500 \end{bmatrix}$$

$$[J3] = \begin{bmatrix} -1.5156 & 0.9920 & 0.5236 \\ 0.9920 & -2.2352 & 1.0443 \end{bmatrix}, \quad [J4] = \begin{bmatrix} 7.9790 & -2.9921 \\ -2.9838 & 8.9513 \end{bmatrix}$$

8. Calculation of voltage angles (degree): Eq. (42).

$$[\theta] = \begin{bmatrix} 0 \\ -7.0100 \\ -6.4337 \\ -2.12350 \end{bmatrix}$$

9. Calculation of linearized power flows (MW): Eq. (6).

$$\begin{bmatrix} P_{1-3} \\ P_{1-4} \\ P_{2-3} \\ P_{2-4} \\ P_{3-4} \end{bmatrix} = \begin{bmatrix} 33.6129 \\ 16.9578 \\ -2.7143 \\ -47.2811 \\ -29.07927 \end{bmatrix}$$

Example:

$$P_{1-3} = 1x0.2 - 0.99459256x0.2 - 0.99459256x(-3)x6.4337x3.14159265/180 = 0.336129 \quad \text{pu}$$

$$P_{1-3} = 0.336129x100 = 33.6129 \quad \text{MW}$$

Table 3 shows the error between the Newton–Raphson power flow output and the DC power flow/linear power flow V-theta calculated for every line in the system by Eqs. (51)–(53).

Table 3 shows the errors obtained with DC power flow/linear power flow V-theta, when Newton–Raphson power flow is used as the reference method. The errors are calculated for every line using Eqs. (51)–(53).

The MW error range of the DC power flow presents an error greater than 2 MW (Eq. (51)) in line number 2 (lines 1–4) Linear power flow V-theta also has the highest error in line 2 and it is 0.92 MW. The largest percentage error in MW is obtained with the DC power flow. The error is calculated at line 4 and it is over 14% (Eq. (52)). The absolute sum of errors in all lines also is largest with the results of DC power flow and it is of 4.14 MW (Eq. (53)).

Table 4
Results of the system of 39 buses.

From bus	To bus	Active power flow Newton full	Active power flow linear V-theta	Active power flow DC	PP_{error} linear V-theta (%)	PP_{error} DC (%)	P_{error} linear V-theta (MW)	P_{error} DC (MW)
9	39	51.5	46.9	46.7	8.93	9.32	4.60	4.80
31	39	52.5	56.7	57.3	−8.00	−9.14	−4.20	−4.80
31	2	−150.1	−154.1	−154.9	−2.66	−3.19	4.00	4.80
2	3	323.1	330.1	335.6	−2.17	−3.87	−7.00	−12.50
2	25	−223.9	−234.5	−240.5	−4.73	−7.41	10.60	16.60
2	30	−250.0	−250.0	−250.0	0.0	0.0	0.0	0.0
3	4	−30.0	−16.3	−14.5	45.67	51.67	−13.70	−15.50
4	5	−296.9	−280.2	−279.9	5.62	5.73	−16.70	−17.00
4	14	−233.3	−235.9	−234.6	−1.11	−0.56	2.60	1.30
5	6	−636.0	−616.8	−615.8	3.02	3.18	−19.20	−20.20
5	8	338.4	337.1	335.9	0.38	0.74	1.30	2.50
6	7	471.7	467.2	466.6	0.95	1.08	4.50	5.10
6	11	−242.5	−256.2	−257.0	−5.65	−5.98	13.70	14.50
6	1	−866.1	−826.9	−825.4	4.53	4.69	−39.20	−40.70
7	8	236.6	232.8	232.8	1.61	1.61	3.80	3.80
8	9	51.8	47.0	46.7	9.27	9.85	4.80	5.10
10	11	260.4	272.5	272.9	−4.65	−4.80	−12.10	−12.50
10	13	389.6	378.8	377.1	2.77	3.21	10.80	12.50
10	32	−650.0	−650.0	−650.0	0.0	0.0	0.0	0.0
13	14	391.1	379.9	378.0	2.86	3.35	11.20	13.10
14	15	155.9	143.0	143.4	8.27	8.02	12.90	12.50
15	16	−164.5	−177.6	−176.6	−7.96	−7.36	13.10	12.10
16	17	132.0	133.3	133.9	−0.98	−1.44	−1.30	−1.90
16	19	−254.0	−260.1	−260.0	−2.40	−2.36	6.10	6.00
16	21	−329.6	−333.3	−334.8	−1.12	−1.58	3.70	5.20
16	24	−42.7	−46.4	−45.1	−8.67	−5.62	3.70	2.40
17	18	128.4	134.9	129.9	−5.06	−1.17	−6.50	−1.50
19	20	374.0	372.5	372.0	0.40	0.53	1.50	2.00
19	33	−629.1	−630.9	−632.0	−0.29	−0.46	1.80	2.90
20	34	−306.9	−307.6	−308.0	−0.23	−0.36	0.70	1.10
21	22	−604.4	−606.8	−608.8	−0.39	−0.73	2.40	4.40
22	23	42.8	42.5	41.2	0.70	3.74	0.30	1.60
22	35	−650.0	−650.0	−650.0	0.0	0.0	0.0	0.0
23	24	353.9	356.2	353.7	−0.65	0.06	−2.30	0.20
23	36	−558.6	−559.4	−560.0	−0.14	−0.25	0.80	1.40
25	26	86.8	82.7	75.5	4.72	13.02	4.10	11.30
25	37	−538.3	−539.3	−540.0	−0.19	−0.32	1.00	1.70
26	27	278.6	283.8	277.0	−1.87	0.57	−5.20	1.60
26	28	−140.8	−145.0	−145.4	−2.98	−3.27	4.20	4.60
26	29	−190.2	−194.4	−195.1	−2.21	−2.58	4.20	4.90
28	29	−347.6	−351.2	−351.4	−1.04	−1.09	3.60	3.80
29	38	−824.8	−827.9	−830.0	−0.38	−0.63	3.10	5.20
Sum of absolute values							266.50	295.60

3. Test results

The proposed method has been applied to several test systems including IEEE systems. This paper presents results of power flow problems in eight systems that are used as traditional tests: Wood and Wollenberg test system (6 buses), New England test system (39 buses), IEEE test systems of 9, 14, 30, 57, 118 and 300 buses. Thus, these stated data systems, are accessible to the international community. All tests whose results are reported in this section have been carried out using three methods of power flows. Newton–Raphson power flow, DC power flow, and linear power flow V-theta. The computer programs were written in MATLAB language, and they use the functions sparse (create sparse matrix), and tic, toc (measure performance using stopwatch timer). We use a computer TOSHIBA, model A505 with 4 processors Intel(R) Core(TM) i7 CPU Q 720 @ 1.60 GHz, subscore 7.0, memory (RAM) 4.00 GB, subscore 5.9, and primary hard disk 207 GB Free (238 GB Total), subscore 6.9.

The results of the full AC power flow and DC power flow, in all simulations, were validated using a power flow software package: Network Analyzer (ANAREDE). The ANAREDE software package is marketed by the Electric Energy Research Center (CEPEL), Brazil.

By storing branch MW flows at final stage of the calculation, a post-solution history of the largest errors in these quantities was constructed. Aiming to analyze the most loaded lines in all our tests, we ignored all flows below of arithmetic mean of load/per bus, except to systems of 39 and 300 buses that present arithmetic mean of load/per bus greater than 78 MW. In these aforesaid systems, the power flows below 30 MW were ignored. Initially we present the results of the power flows and errors in lines with the system of 39 buses (New England power system). This system has the highest arithmetic mean of load/per bus, which is of 160.4 MW/per bus.

Table 4 shows the errors obtained with DC power flow/linear power flow V-theta, when Newton–Raphson power flow is used as the reference method. The errors are calculated for every line using Eqs. (51)–(53). The system buses were renumbered and the bus number one is the swing bus.

It is possible to observe that the largest absolute percentage error of the DC power flow occurs along the lines 3–4 and it is 51.67%. The largest absolute percentage error of power flow linear V-theta occurs on the lines 3–4, which is 45.67%. The biggest error in MW can occur on a line different from the largest percentage error. Therefore, the largest absolute error of the DC power flow in MW occurs on the lines

Table 5
Errrors due linear power flow solution.

No. of buses in system	Linear power flow V-theta			DC power flow		
	Max(abs(P_{error})) (MW)	Max(abs(PP_{error})) (%)	PA_{error} (MW)	Max(abs(P_{error})) (MW)	Max(abs(PP_{error})) (%)	PA_{error} (MW)
6[c]	0.74	1.70	1.38	2.49	7.01	5.66
9[a]	4.26	5.96	8.97	4.54	6.34	9.28
14[a]	7.36	4.69	12.98	8.95	5.87	23.76
30[a]	9.22	5.32	19.56	12.23	9.53	37.31
39[b]	39.20	45.67	266.50	40.70	51.67	295.60
57[a]	6.08	5.95	36.78	9.57	12.61	72.28
118[a]	49.75	39.58	317.11	60.61	48.22	393.95
300[a]	360.32	155.45	3210.3	402.92	173.02	3684.1

[a] IEEE Standard Test System.
[b] New England system. Max(abs) is the maximum absolute value.
[c] Wood and Wollenberg system.

Table 6
Comparison of errors in terms of lines.

No. of buses in system	No. of lines with MW > power flows ignored	No. of lines with error lpf V-theta MW < error power flow dc MW	Corresponding (%)
6	3	3	100
9	7	5	71.43
14	10	9	90.00
30	19	18	94.74
39	42	34	80.95
57	23	17	73.91
118	86	63	73.26
300	278	193	69.42

lpf V-theta – linear power flow V-theta.

6–1 and it is 40.70 MW. The highest absolute error of linear power flow V-theta also occurs on the lines 6–1, and it is 39.20 MW. The sum of absolute errors in the DC power flow is 295.60 MW, while this sum in the linear power flows is 266.50 MW.

The linear power flow V-theta performs better than the DC power flow in 34 of a total of 42 lines, which is shown in Table 4. On the eight lines, where the DC power flow produces better results, the differences in favor (absolute value of MW) of the DC power flow, are small: lines 4–14 → 1.3; lines 14–15 → 0.4; lines 15–16 → 1; lines 16–19 → 0.1; lines 16–24 → 0.7; lines 17–18 → 5; lines 23–24 → 2.1 and lines 26–27 → 3.6. While we consider the eight errors, where the linear power flow V-theta produces better results, the differences in favor (absolute value of MW) of the linear power flow V-theta, are higher than the values previously: lines 2–3 → 5.5; lines 2–25 → 6; lines 3–4 → 1.8; lines 6–1 → 1.5; lines 10–11 → 1.7; lines 13–14 → 1.9; lines 16–21 → 1.5 and lines 21–22 → 2.

Table 5 presents a summary of the largest absolute error in percentages, as well as the largest absolute error in MW, in each of the simulated systems.

As can be seen in Table 5, in all systems the largest absolute error in percentage and MW are due to the DC power flow. As well as the absolute sum of errors in the lines is greater for the results obtained with the DC power flow. In Table 5, the system of 300 buses had the highest error both in MW and in percentage. The biggest error (MW) occurs in line 7049-49. In this line DC power flow has a reverse flow. The flow in this line obtained by using the Newton–Raphson power flow is 372.72 MW, the value obtained by the DC power flow is −30.2 MW (negative value) and the value obtained by the linear power flow V-theta is of 12.4 MW (positive value).

Table 6 presents a comparison of errors in terms of lines for all systems simulated.Table 6 shows that in most lines the linear power flow V-theta has better performance than the DC power flow. On lines where it does not, a situation similar to that seen in the system of 39 buses occurs, i.e. the differences in favor (absolute value of MW) of the DC power flow are small as can be seen in the Figs. 2 and 3. These figures show the profile of errors for the system of 57 buses and to system of 118 buses in MW.

As can be seen clearly in the figures cited the results obtained with the DC power flow shows the highest levels of errors.

We can see in Table 7, the total computing times for the systems simulated in the paper.

DC power flow is faster than linear power flow V-theta, as it was expected. However, the simulation times are acceptable, due to the linear power flow V-theta. Today, there are computers faster than the computer used in the simulations. Therefore, the computing time may be lower.

Table 7
Total computing time.

Power system		Computing time (s)	
No. of buses	No. of branches	DC power flow	Linear power flow V-theta
6	11	0.0023	0.0844
9	9	0.0023	0.0845
14	20	0.0025	0.0904
30	41	0.0028	0.0999
39	46	0.0029	0.1066
57	80	0.0031	0.1143
118	186	0.0050	0.1824
300	411	0.0189	0.6819

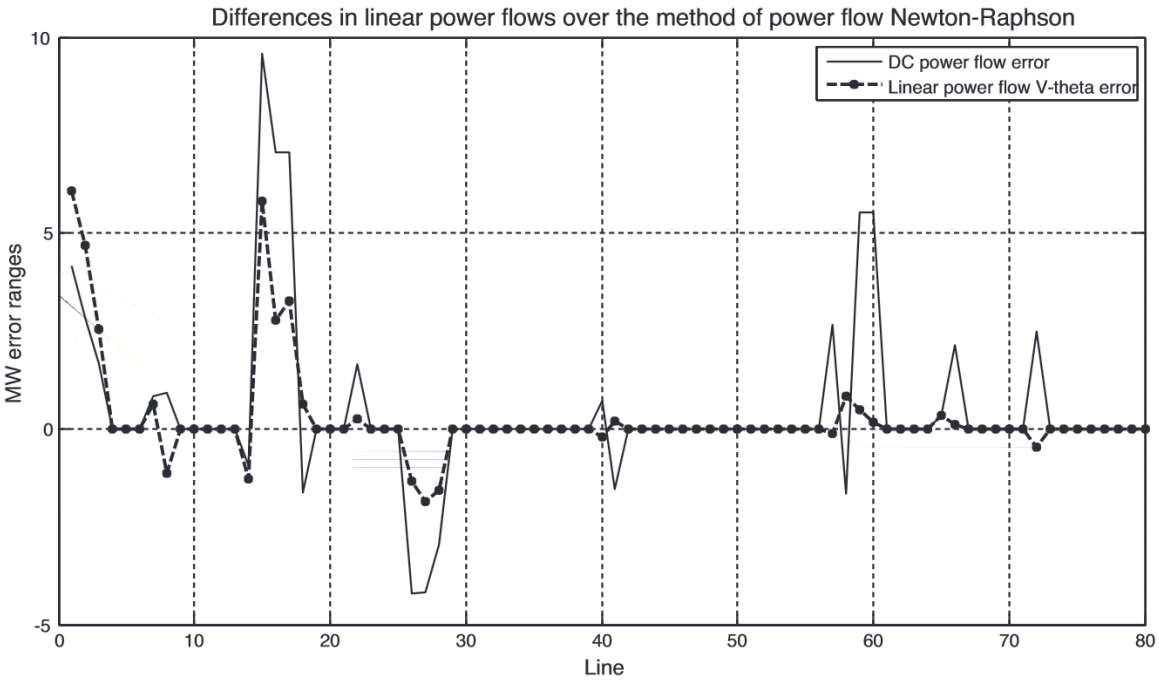

Fig. 2. Active power flow (MW) error – IEEE 57 test system.

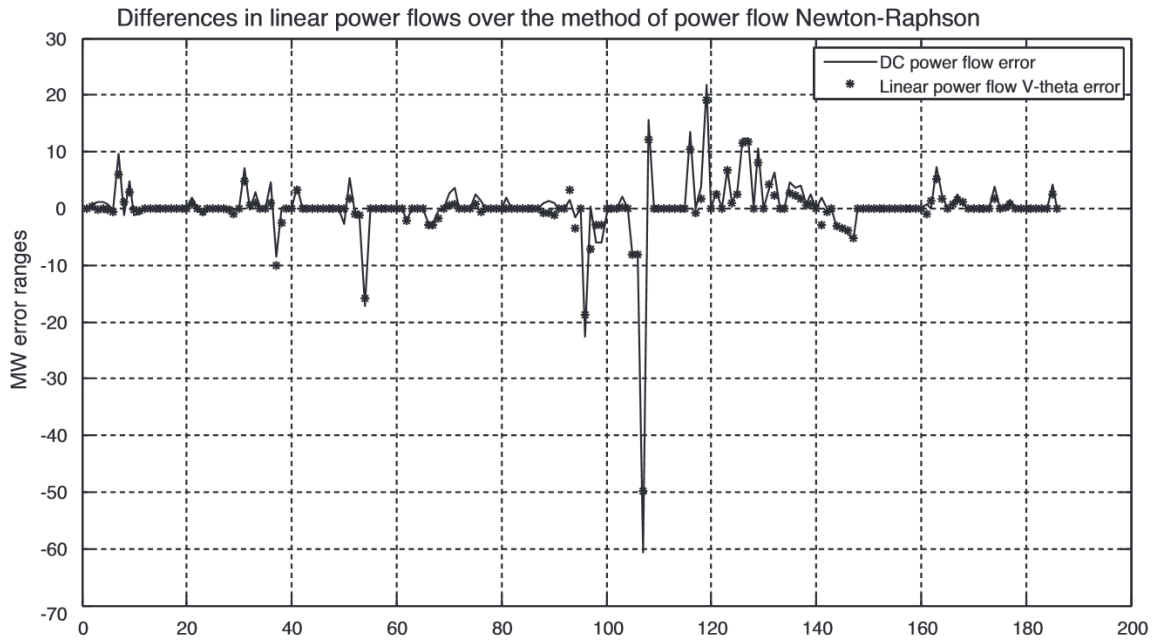

Fig. 3. Active power flow (MW) error – IEEE 118 test system.

4. Conclusions

A novel linear power flow method is developed in this paper. This proposed method calculates the voltage magnitudes decoupled from the voltage angles. The new linear decoupled power flow method was tested together with the original DC power flow method, using various systems, including the IEEE test systems, compared with the Newton AC full power flow solution. The proposed method herein, is superior to the classical DC power flow. The results from the new method gave very encouraging results in terms of "errors" in the line power flows, compared to the traditional dc method. It is expected that this new method could be applied to many applications in power systems, where the traditional DC method is now used.

Appendix A.

A.1. DC power flow

DC power flow is a linear problem. It neglects active power losses, and assumes that magnitudes of nodal voltages are equal. Furthermore, voltage angle differences are assumed to be small. The only variables are voltage angles and active power injections. Due to the fact that losses are neglected, all active power injections are known in advance. Therefore the problem becomes linear and there is no need for iterations. Consider expressions for the active power flows (P_{km} and P_{mk}) in a transmission line:

$$P_{km} = V_k^2 g_{km} - V_k V_m g_{km} \cos \theta_{km} - V_k V_m b_{km} \sin \theta_{km} \tag{54}$$

$$P_{mk} = V_m^2 g_{km} - V_m V_k g_{km} \cos \theta_{km} + V_m V_k b_{km} \sin \theta_{km} \tag{55}$$

If the terms corresponding to the active power losses are ignored, in Eqs. (54) and (55), the result is:

$$P_{km} = -P_{mk} = -V_k V_m b_{km} \sin \theta_{km} \tag{57}$$

The following additional approximations are often valid. $V_k \cong V_m \cong 1$ p.u., $\sin \theta_{km} \cong \theta_{km}$ and $b_{km} \cong -(1/x_{km})$
Using these approximations to simplify the expression for the active power flow P_{km} yields

$$P_{km} = x_{km}^{-1} \theta_{km} = \frac{\theta_k - \theta_m}{x_{km}} \tag{58}$$

However, such approximations are not always realistic. Firstly, the X/R ratio condition can be difficult to guarantee. The influence of resistance increases with the decrease of voltage, which means that only the high voltage transport networks can withstand this condition. Moreover, voltages will most likely not be flat but will vary among buses, causing the voltage profile to be different from the assumed one. Each of these assumptions has some influence on the accuracy of the power flow calculations [15].

References

[1] J. Duncan Glover, M.S. Sarma, T.J. Overbye, Power System Analysis and Design, 5th ed., Thomson Learning, 2011.
[2] A.M. Leite da Silvaa, J.G.C. Costaa, L.A.F. Mansob, G.J. Andersc, Evaluation of transfer capabilities of transmission systems in competitive environments, Electrical Power and Energy Systems (2004 May) 257–263.
[3] A. Ivan, Skokljev, V. Dejan, ToSiC, A new symbolic analysis approach to the DC load flow method, Electric Power Systems Research (1997 February) 127–135.
[4] Shuai Lu, Ning Zhou, Nirupama Prakash Kumar, Nader Samaan, B. Bhujanga, Chakrabarti, Improved dc power flow method based on empirical knowledge of the system, Proceedings of IEEE PES. Transmission and Distribution Conference and Exposition (2010 April) 1–6.
[5] Y.-H. Song, X.-F. Wang, Operation of Market-oriented Power Systems, Springer, 2010.
[6] A.J. Wood, B.F. Wollenberg, Power Generation Operation and Control, 3rd ed., Wiley-InterScience, New York, 2011.
[7] K. Purchala, L. Meeus, D.V. Dommelen, R. Belmans, Usefulness of dc power flow for active power flow analysis, in: Proceedings of IEEE PES General Meeting, San Francisco, CA, USA, June, 2005, pp. 1–6.
[8] B. Stott, J. Jardim, O. Alsaç, DC power flow revisited, in: IEEE Trans. Power Syst., 2009 August, pp. 1290–1300.
[9] O. Alsaç, J. Bright, S. Brignone, M. Prais, C. Silva, B. Stott, N. Vempati, FTRs-The rights to hedge congestion costs, in: IEEE Power Energy Mag., 2004 July/August, pp. 47–57.
[10] T.J. Overbye, X. Cheng, Y. Sun, A comparison of the AC and DC power flow models for LMP calculations, in: Proc. 37th Hawaii Int. Conf. System Sciences Waikoloa, Hawaii, 2004.
[11] S. Grijalva, P.W. Sauer, J.D. Weber, Enhancement of linear ATC calculations by the incorporation of reactive power flows, in: IEEE. Trans. Power Syst., 2003 May, pp. 619–624.
[12] W.G. McCallum, D. Hughes-Hallett, A.M. Gleason, D.O. Lomen, D. Lovelock, J. Tecosky-Feldman, T.W. Tucker, D.E. Flath, J. Thrash, K.R. Rhea, A. Pasquale, S.P. Gordon, D. Quinney, P.F. Lock, Multivariable Calculus, John Wiley & Sons Inc, USA, 1997.
[13] A.J. Monticelli, State Estimation in Electric Power Systems, Kluwer Academic Publishers, USA, 1999.
[14] Gareth Williams, Overdetermined systems of linear equations, The American Mathematical Monthly (1990 June–July) 511–513.
[15] L. Powell, Power System Load Flow Analysis, McGraw-Hill Professional Series, New York, 2004.